CAMBRIDGE
UNIVERSITY PRESS

## Article

# Mineralogy of the baotite-bearing Gundrapalli lamproite, Nalgonda district, Telangana, India

Gurmeet Kaur[1,2]* and Roger H. Mitchell[2]

[1]Department of Geology, Panjab University, Chandigarh UT-160014, India; and [2]Department of Geology, Lakehead University, Thunder Bay Ontario, Canada P7B 5E1

### Abstract

We describe the mineralogy of a lamproite dyke from Gundrapalli village (Nalgonda district), Telangana, India. The dyke consists of a mineral assemblage characteristic of lamproites in terms of the presence of amphiboles (mainly potassic-richterite together with potassic-arfvedsonite, magnesio-riebeckite, Ti-rich potassic-magnesio-arfvedsonite, potassic-magnesio-arfvedsonite, katophorite and potassic-ferri-katophorite), Al-poor pyroxene, phlogopite (Ti-rich, Al-poor), pseudomorphed leucite, spinel (chromite-magnesiochromite), fluorapatite, baryte, titanite, rutile, barytocalcite, calcite, ilmenite, hydro-zircon, baotite, strontianite, allanite, quartz and pyrite. The absence of wadeite and priderite have been compensated for by the presence of baotite, rutile, titanite, baryte and hydro-zircons. The presence of the secondary phases: allanite, hydro-zircon, chlorite, quartz and cryptocrystalline silica, implies that the dyke has undergone deuteric alteration. On the basis of its typomorphic mineralogy the Gundrapalli dyke has been classified as a pseudoleucite-phlogopite-amphibole-lamproite. We report the presence of the rare mineral baotite from this lamproite, the first recognition of baotite from a lamproite in India. The mineralogy of the baotite-bearing Gundrapalli lamproite is analogous to the baotite-bearing Kvaløya lamproite from Troms, Norway.

## Introduction

Lamproite magmas commonly originate in the upper mantle at depths ranging from the sub-continental lithospheric mantle to the asthenospheric mantle. They are commonly enriched in volatiles (Mitchell and Bergman, 1991; Tainton and McKenzie, 1994; Mitchell, 1995; Murphy *et al.*, 2002; Davies *et al.*, 2006; Rapp *et al.*, 2008; Mitchell and Tappe, 2010, Tappe *et al.*, 2007, 2013). Lamproite rocks are reported from subduction environments and within-plate cratonic regions (Mitchell and Bergman, 1991; Mitchell, 1995; Nowell *et al.*, 2004; Prelević *et al.*, 2008; Tommasini *et al.*, 2011; Fritschle *et al.*, 2013; Gurmeet Kaur *et al.*, 2018 and references therein).

Lamproites are hybrid rocks which are best characterised by detailed mineralogical studies (Mitchell and Bergman, 1991; Mitchell, 2006 and references therein). Lamproites contain typomorphic minerals such as: phlogopite (alumina poor phenocrysts, tetraferriphlogopite groundmass); titanian potassium richterite; forsteritic olivine; Al- and Na-poor diopside; leucite; and sanidine. In addition to the major minerals, lamproites are also characterised by the presence of accessory minerals: priderite; wadeite; apatite; perovskite; titanian-magnesiochromite; magnesio-chromite; magnesian titaniferous magnetite; jeppeite; armalcolite; shcherbakovite; ilmenite; and enstatite (Mitchell and Bergman, 1991; Mitchell, 1995; Woolley *et al.*, 1996). Mineralogical studies

of lamproites are significant as they reflect the nature of the parental magma. Lamproite rocks with priderite, wadeite, jeppeite, armalcolite and shcherbakovite are indicative of derivation of lamproite from magmas enriched in incompatible and large-ion-lithophile elements. The presence of K-Ba titanites and K-Zr silicates also distinguishes lamproites from archetypal (or Group-I) kimberlites. The distinction between lamproites and kimberlites can be made on the basis of the presence of typomorphic minerals (Mitchell and Bergman, 1991; Mitchell, 1995). Following the mineralogical-genetic classification proposed by Mitchell (1995) and Mitchell and Bergman (1991), we classify the dyke occurring at Gundrapalli in the Ramadugu Lamproite field of Telangana in the Eastern Dharwar Craton as a *bona fide* lamproite. We also compare the mineralogy of the Gundrapalli dyke with the Kvaløya lamproite from Troms, Norway.

## Eastern Dharwar Craton lamproites

The Dharwar Craton of southern India comprises two blocks: The Eastern and the Western Dharwar blocks. The Eastern Dharwar block is known for numerous occurrences of kimberlites and lamproites, whereas there are to date no reports of these rocks from the Western Dharwar block (Fig. 1; Neelkantam, 2001; Fareeduddin and Mitchell, 2012 and references therein). The lamproite fields in the Eastern Dharwar block are: (1) the Wajrakarur field with the P2-West, P12, P5, P13, P4, TK1 and TK4 intrusions which were classified formerly as kimberlites, but have been reclassified recently as lamproites (Gurmeet Kaur *et al.*, 2013; Gurmeet Kaur and Mitchell, 2013; Gurmeet Kaur and Mitchell,
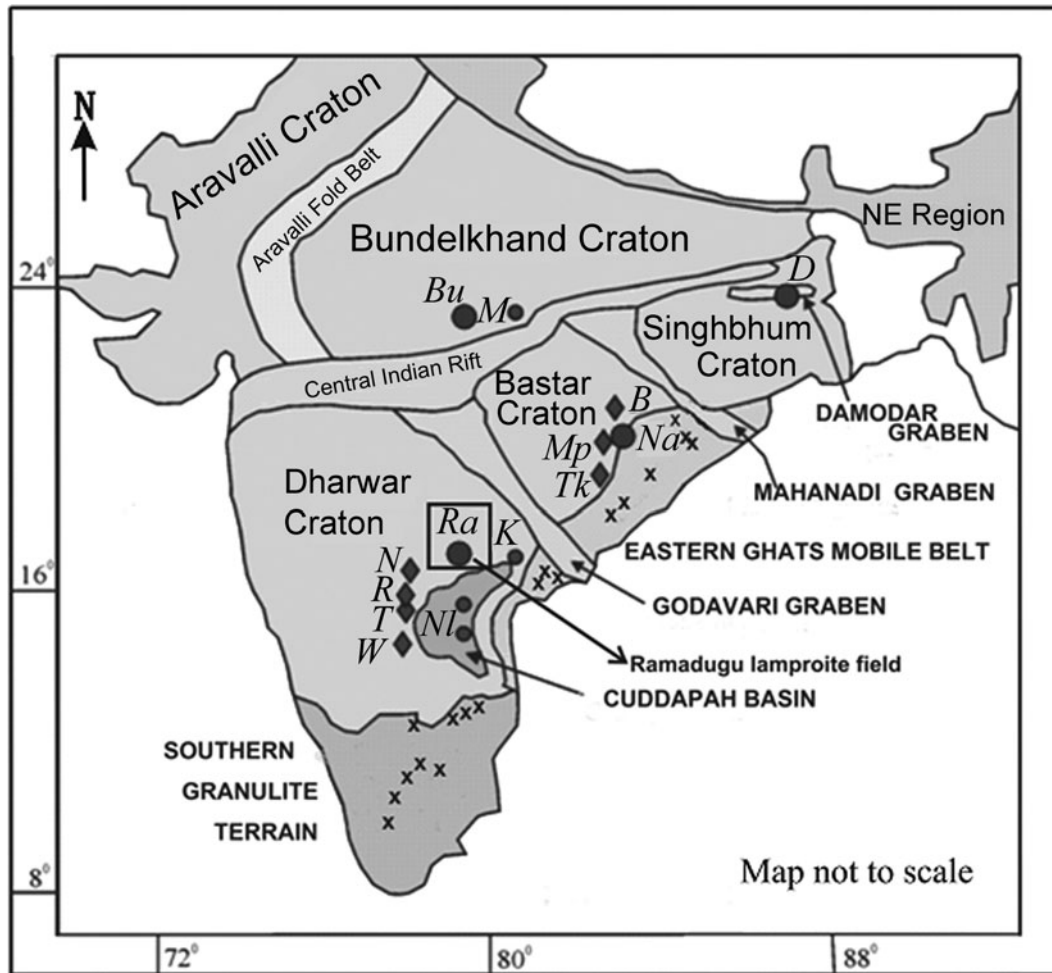
**Fig. 1.** Distribution of kimberlites and lamproites in the Bundelkhand, Singhbhum, Bastar and Dharwar cratons of the Indian subcontinent. Diamonds (◊), circles (o) and crosses (x) refer to kimberlites, lamproites and deformed alkaline rocks and carbonatites (DARC) locations in the southern Indian sub-continent, respectively. Bu – Bunder lamproites; M – Majhgawan lamproite field; B – Basna kimberlite field; Na – Nawapara lamproite field; Mp – Mainpur kimberlite field; Tk – Tokapal kimberlite field; Ra – Ramadugu lamproite field; N – Narayanpet kimberlite field; R – Raichur kimberlite field; T – Tungabhadra kimberlite field; W – Wajrakarur kimberlite field; Nl – Nallamalai lamproite field; K – Krishna lamproite field; and D – Damodar valley lamproites (Gurmeet Kaur and Mitchell, 2016; Gurmeet Kaur et al., 2018).

2016; Shaikh et al., 2017; Shaikh et al., 2018); (2) the Cuddapah Basin lamproites with the Chelima, Zangamarajupalle, Garledinne, Banganapalle intrusions (Chalapathi Rao et al., 2004; Chalapathi Rao et al., 2016 and references therein); (3) the Krishna lamproite field (Chalapathi Rao et al., 2010 and references therein); and (4) the Ramadugu lamproite field (Chalapathi Rao et al., 2014; Gurmeet Kaur et al., 2016; Gurmeet Kaur and Mitchell, 2017; Gurmeet Kaur et al., 2018 and references therein). The Eastern Dharwar block lamproite emplacement/event preceded the global kimberlite event at 1.1 Ga (Kumar et al., 2007; Tappe et al., 2018a; Talukdar et al., 2018 and references therein). The Eastern Dharwar block lamproites range in age from 1.25 to 1.4 Ga (Chalapathi Rao et al. 2013; Talukdar et al., 2018 and references therein). The Mesoproterozoic kimberlites and lamproites have a strong bearing on the diamond prospectivity in the global context (Kumar et al., 2007; Farreddudin and Mitchell, 2012; Tappe et al., 2018b). Talukdar et al. (2018) elaborate on the comparable mineralogical, trace element, and isotopic geochemical affinity of the Eastern Dharwar block lamproites and relate their emplacement to dispersal of the Columbia supercontinent during the Mesoproterozoic period.

## Ramadugu lamproite field

The Ramadugu lamproite field occurs in the Telangana state of India. It lies NNW of the Cuddapah Basin and is located close to the Krishna lamproite field (Fig. 1). The Ramadugu lamproite field consists of dykes located in the villages of Ramadugu, Somavarigudem, Yacharam, Vattikod, Gundrapalli and Marepalli (Fig. 2). The Ramadugu dykes are emplaced in the Peninsular Gneissic Complex of the Eastern Dharwar block (Fig. 2; Sridhar and Rau, 2005; Ahmed and Kumar, 2012; Kumar et al., 2013; Chalapathi Rao et al., 2014; Gurmeet Kaur et al., 2018). The Gundrapalli dyke of the Ramadugu lamproite field was discovered by Ahmed and Kumar (2012).

## Gundrapalli dyke

The Gundrapalli dyke is intrusive into the granite unit of Peninsular Gneissic Complex (Fig. 2). It extends in the NW–SE direction and is traceable up to an approximate length of 93 m with thickness of the dyke varying from 70 to 100 cm. The dyke is not continuous and the outcrops are rarely visible because
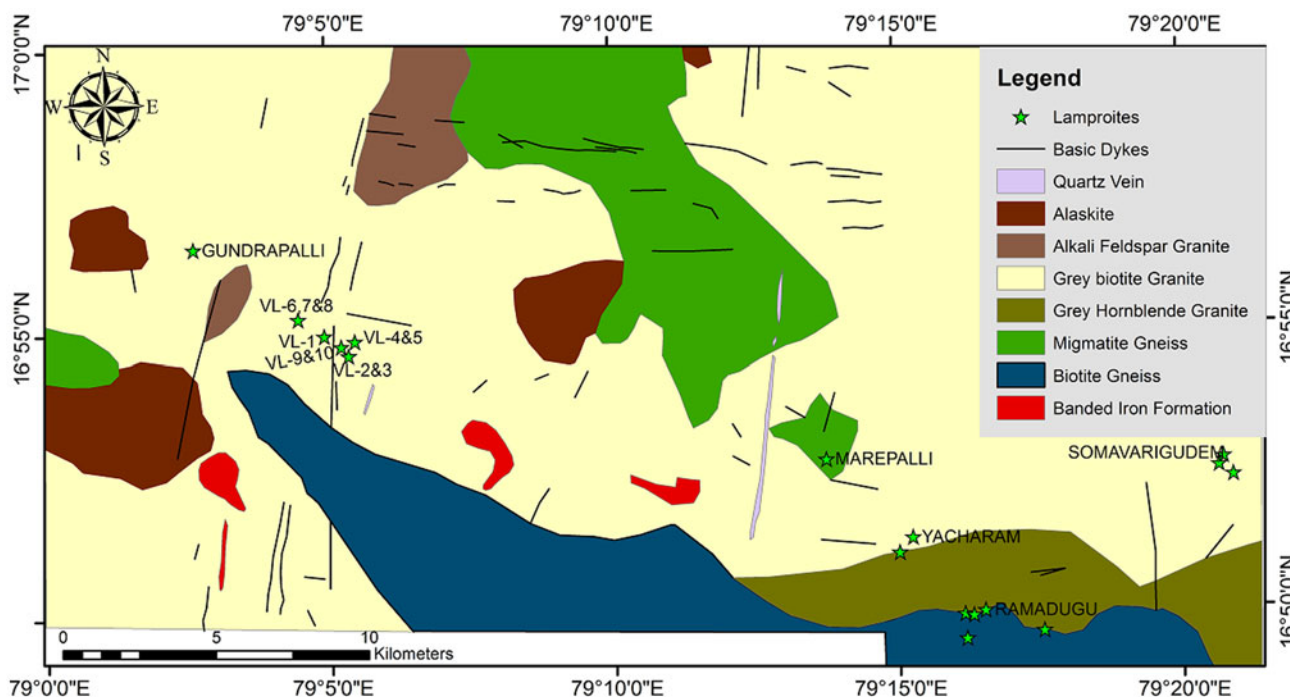
**Fig. 2.** Ramadugu lamproite field marked with the Ramadugu, Yacharam, Somavarigudem and Vattikod lamproite dykes, Nalgonda district, Telangana, India. The location of Gundrapalli lamproite and other Ramadugu lamproite dykes are also marked with a star.

of concealment of the dyke beneath the soil and vegetation cover (Fig. 3a). The rock in the field appears greyish black in colour and altered (Fig. 3b). The Gundrapalli dyke lies in close proximity to the Vattikod lamproite dyke system (Fig. 2; Kumar *et al.*, 2013; Gurmeet Kaur *et al.*, 2018). Field records and preliminary work on the Gundrapalli dyke can be found in the Geological Survey of India (GSI) report by Ahmed and Kumar (2012) available on the GSI website (www.portal.gsi.gov.in). This paper presents a detailed mineralogical study of the Gundrapalli dyke and provides textural and compositional data for major, minor and accessory minerals. These data are used to identify conclusively the Gundrapalli dyke as lamproite.

## Analytical techniques

Gundrapalli dyke rock samples were investigated by back-scattered electron (BSE) imagery and quantitative energy dispersive X-ray spectrometry. The compositional data for the minerals were obtained by standard quantitative X-ray energy dispersive spectrometry using a Hitachi SU-70 field emission Scanning Electron Microscope (SEM) and the Oxford Instruments AZtec analysis system at Lakehead University, Thunder Bay, Canada. Acceleration voltage was 20 kV with a beam current of 300 pA. Standards used were those given by Liferovich and Mitchell (2005): synthetic pyroxene glass DJ35 (Si, Ca); corundum (Al); jadeite (Na,Al), $BaF_2$ (Ba, F), Mn 'hortonolite' (Mg, Fe Si, Mn); apatite (P); $SrTiO3$ (Sr, Ti), $ThNb_4O_{12}$ (Th, Nb); ilmenite (Ti, Fe), gahnite (Zn) and zircon (Zr). Accuracy for major (> 10 wt.%) elements was typically better than (+/−1%) and for minor elements (from 1 and 10 wt.%) was (+/−2%), and was assessed by replicate analysis of standards against each other. Relative standard deviations for minor and major elements was < +/−3%, +/−2% and < +/−1% for elements occurring at < 1 wt.%, 1–10 wt.% and > 10 wt.% oxide. The small beam size and low

beam currents employed ensured accurate analysis of small grains without excitation of adjoining material.

## Petrography and mineralogy of Gundrapalli dyke

The Gundrapalli dyke consists of apatite phenocrysts and micro-phenocrysts set in generally fine grained groundmass. It also contains phenocrysts and microphenocrysts of pseudoleucite. Apatite is the only unaltered phenocryst and microphenocryst phase in addition to being a common groundmass mineral (Figs 4a–b, 5a). The former leucite phenocrysts are pseudomorphed by potassium feldspar, calcite, quartz and cryptocrystalline silica (Fig. 5b). The fine-grained groundmass consists of potassium-rich amphiboles, tetraferriphlogopite, Na- and Al-poor clinopyroxene, potassium-feldspar (pseudoleucite), spinel, apatite, calcite, baryte, titanite, rutile, allanite and baotite (Figs 5a–d and 6a–d). Minor phases are magnetite, pyrite and hydro-zircon (Figs 5c and 6c).

Amphibole is the commonest groundmass phase. It mostly occurs as prismatic and wedge-shaped crystals (Figs 5c–d). Commonly associated accessory phases are titanite, rutile, hydro-zircons, calcite, pyroxene, chlorite and baotite (Figs 5b–d). Representative compositions of amphibole are given in Table 1. The amphiboles have low $Al_2O_3$ (<0.5 wt.%) contents, and contain (9.04 to 0.70 wt.%) $TiO_2$, (6.66 to 3.87 wt.%) $Na_2O$, (5.55 to 2.25 wt.%) $K_2O$, and (20.20 to 8.64 wt.%) $FeO_T$. The amphiboles are compositionally diverse and include: potassic-richterite, potassic-arfvedsonite, magnesio-riebeckite, Ti-rich potassic-magnesio-arfvedsonite, potassic-magnesio-arfvedsonite, katophorite and potassic-ferri-katophorite. The majority are potassic-richterite typical of lamproite rocks (Table 1). The extremely low $Al_2O_3$ contents are characteristic of lamproite amphiboles (Mitchell and Bergman, 1991) and such low contents of alumina are primarily related to the parental peralkaline nature of magma (Wagner and Velde, 1986; Mitchell and Bergman, 1991).

The second most abundant groundmass mineral is potassium feldspar. The typical habit of the feldspar indicates that it represents pseudomorphs after former leucite (Fig. 5a) and fresh leucite is not observed in the Gundrapalli dyke. The potassium feldspar pseudomorphs also contain calcite, hydro-zircons and quartz, minerals which are also found in leucite pseudomorphs in the Vattikod lamproites (Gurmeet Kaur et al., 2018). The pseudomorphs are also cross-cut by cryptocrystalline silica veinlets (Fig. 5b). Representative compositions of potassium feldspar (Table 2) show that they are relatively poor in $Na_2O$ (n.d.–0.24 wt.%) and $FeO_T$ (n.d.–0.62 wt.%), and similar to potassium feldspars in other lamproites (Mitchell and Bergman, 1991; Kumar et al., 2013 and Gurmeet Kaur et al., 2018).

Phlogopite, a minor groundmass phase, is typically tetraferriphlogopite characteristic of lamproites (Fig. 6c). Representative
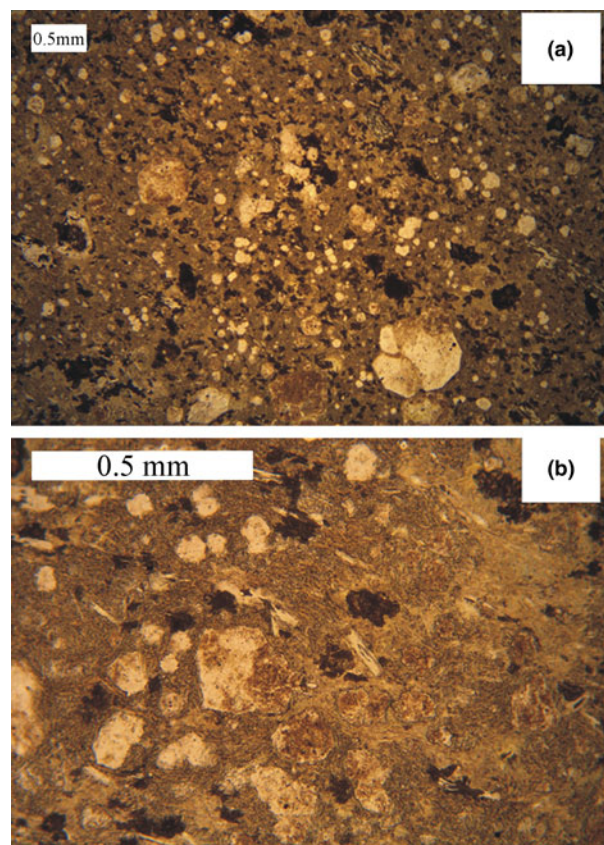


**Fig. 4.** Plane-polarised light images of (a) the inequigranular texture of the Gundrapalli dyke; and (b) greenish-brown prismatic amphiboles and ovoid pseudo-leucites in a fine grained matrix (PPL)

compositions (Table 3) show that they are poor in $Al_2O_3$ (8.66–5.54 wt.%) and enriched in $FeO_T$ (19.91–17.63 wt.%) and $TiO_2$ (5.99–4.14 wt.%), with the fluorine contents varying from 1.83–1.11 wt.%. The low $Al_2O_3$ contents of Gundrapalli groundmass phlogopites compare well with the range of 5–11 wt.% $Al_2O_3$ defined for lamproite phlogopites (Mitchell, 1989; Mitchell and Bergman, 1991). The BaO contents are <2 wt.%.

Clinopyroxene is not commonly present in the Gundrapalli dyke. It occurs as an accessory phase and commonly is altered to chlorite. Representative compositions (Table 4), show that the clinopyroxene are poor in $Al_2O_3$ (0.77–0.66 wt.%) and $Na_2O$ (0.77–0.53 wt.%). The pyroxenes from Gundrapalli differ from those in the nearby Vattikod lamproites which are extremely enriched in $FeO_T$ up to 17 wt.% (Gurmeet Kaur et al., 2018).

Apatite occurs as a phenocrystal-to-microphenocrystal and groundmass phase (Fig. 5a). The phenocrystal apatite occurs as euhedral-to-elongated crystals which are zoned compositionally (Fig. 6d). The apatites occur in association with groundmass amphibole, titanite, rutile, calcite, baotite and hydro-zircon. Representative compositions (Table 5), indicate that they are rich in SrO (up to 3.59 wt.%) and fluorine (up to 3.77 wt.%), and can be classified as fluorapatites. The apatites which are zoned are typically impoverished in SrO and F in the core and are enriched in SrO and F at their rims (Table 5).

Spinel occurs as an accessory groundmass phase forming zoned, euhedral-to-subhedral crystals (<50 μm). Rutile is a late-stage phase associated with titanite. Rutile, although not a common and representative phase of lamproites, has been reported
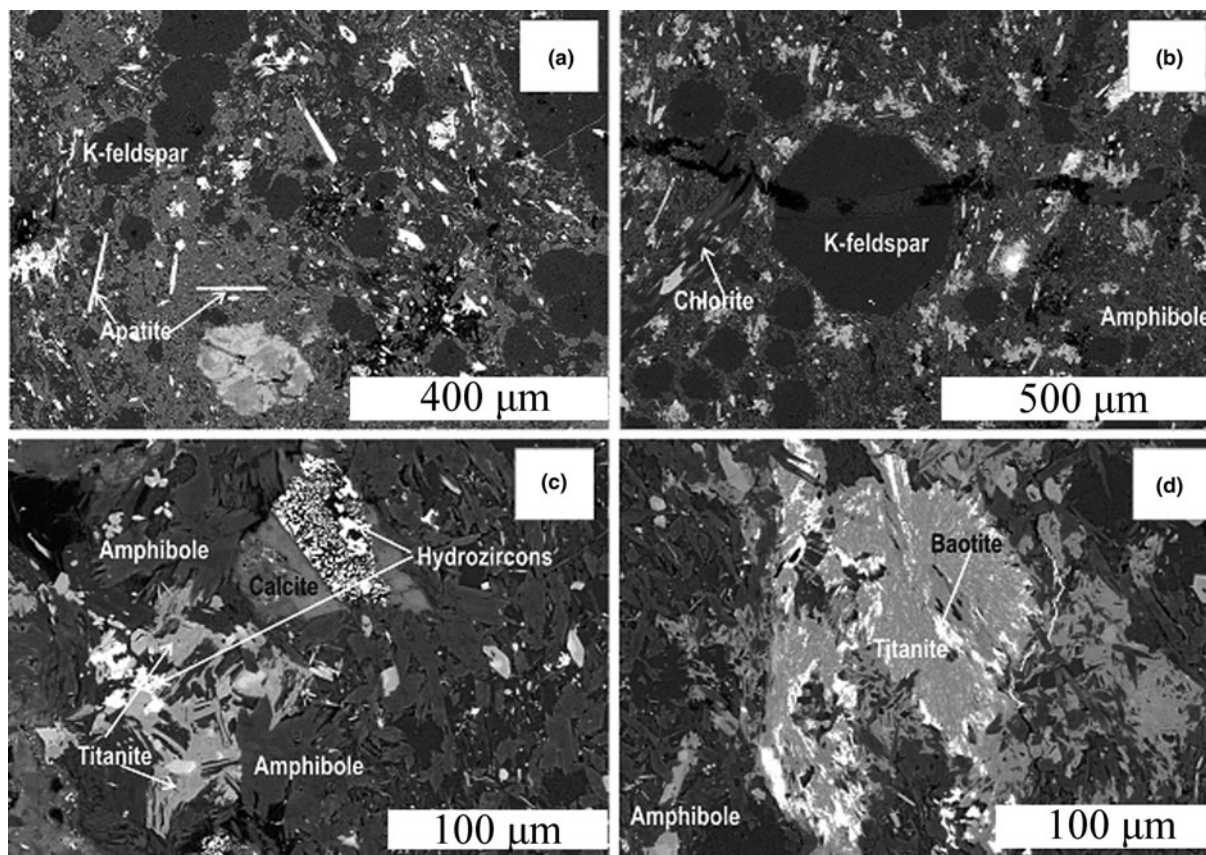
**Fig. 5.** Back-scatter electron images of: (*a*) the inequigranular texture of the dyke with acicular apatite and pseudoleucite; (*b*) a veinlet of cryptocrystalline silica and chlorite cross-cutting the K-feldspar pseudomorph; (*c*) amphiboles, titanites, calcite and hydro-zircons in the Gundrapalli lamproite (the upper centre part shows the hydro-zircons and calcite association); and (*d*) acicular baotite forming together with titanite.

previously from some Indian lamproites (Mitchell and Fareeduddin, 2009; Chalapathi Rao *et al.*, 2014; Gurmeet Kaur *et al.*, 2018). The other accessory groundmass phases are: titanite, allanite, calcite, baryte, hydro-zircon and baotite (Figs 5*c*–*d* and 6*b*–*d*). Titanite occurs as aggregates and is mainly associated with amphibole, rutile and baotite. Titanites have also been reported from other Indian lamproites (Chalapathi Rao *et al.*, 2014; Gurmeet Kaur *et al.*, 2018). Calcite is commonly present as a late-stage residual groundmass phase. It also occurs as secondary pseudomorphs after earlier-crystallised mineral leucite together with K-feldspar and quartz. Baryte occurs as a late-stage mineral and also commonly seen as small veinlets cross-cutting the rock. Hydro-zircons occur in the cores of pseudomorphed leucite as aggregates of very fine grains. Chlorite forms as a replacement product of groundmass amphibole, pyroxene and phlogopite. Aggregates of quartz are common in pseudomorphed leucite. Cryptocrystalline veins of silica commonly cross-cut the rock as a late-stage phase. The rare mineral baotite forms aggregates with radiating structures and is closely-associated with rutile, amphiboles and titanite (Figs 5*d* and 6*a*–*b*). Baotite compositions are given in Table 6.

## Baotite from peralkaline, alkaline and other associated rocks

Baotite, chlorine bearing Ba-Ti-(Nb) silicate, is a rare mineral commonly reported from peralkaline, alkaline and associated rocks. Generally, baotites from different rock types have compositions varying between the end-members $Ba_4Ti_8Si_4O_{28}Cl$ and $Ba_4Ti_2Fe_2^{2+}Nb_4Si_4O_{28}Cl$ (Kullerud *et al.*, 2012 and references therein). Baotite was reported for the first time from hydrothermal quartz veins of the Bayan-Obo mine of Mongolia, China (Peng, 1959; Semenov *et al.*, 1961). Subsequently, baotite has been reported from rocks which mostly belong to the alkaline/peralkaline and carbonatite series. Some of the important world occurrences of baotites from alkaline/peralkaline and carbonatite series rocks are (Kullerud *et al.*, 2012 and references therein): (1) carbonatites and carbonatite veins and dykes from US, Russia, Democratic Republic of Congo and New Zealand (Heinrich *et al.*, 1962; Koneva *et al.*, 2008; Wall *et al.*, 1996; Cooper, 1996); (2) alkali-granite pegmatites and hydrothermal rocks from Pakistan; Tajikistan (Obodda and Leavens, 2004; Karpenko and Pautov, 2002); (3) lamproites from Russia, Czech Republic, Norway and India (Rudashevsky *et al.*, 2011; Nemec, 1987; Krmíček *et al.*, 2011; Kullerud *et al.*, 2012; Gurmeet Kaur and Mitchell, 2017); and (4) alkaline pegmatites from United States (Chakhmouradian and Mitchell, 2002). Table 7 summarises the wide geographic distribution and compositional range of baotites.

The rare occurrence of baotite and few petrographic studies, together with limited knowledge on the nature of late-stage fluids associated with them in particular and alkaline/peralkaline rocks in general precludes a complete understanding of formation of baotite in different rocks from different environments. The common factors in the genesis of baotites in different environments are: (1) baotites are mostly associated with alkaline/peralkaline rocks; and (2) baotites form as a late-phase liquidus mineral in
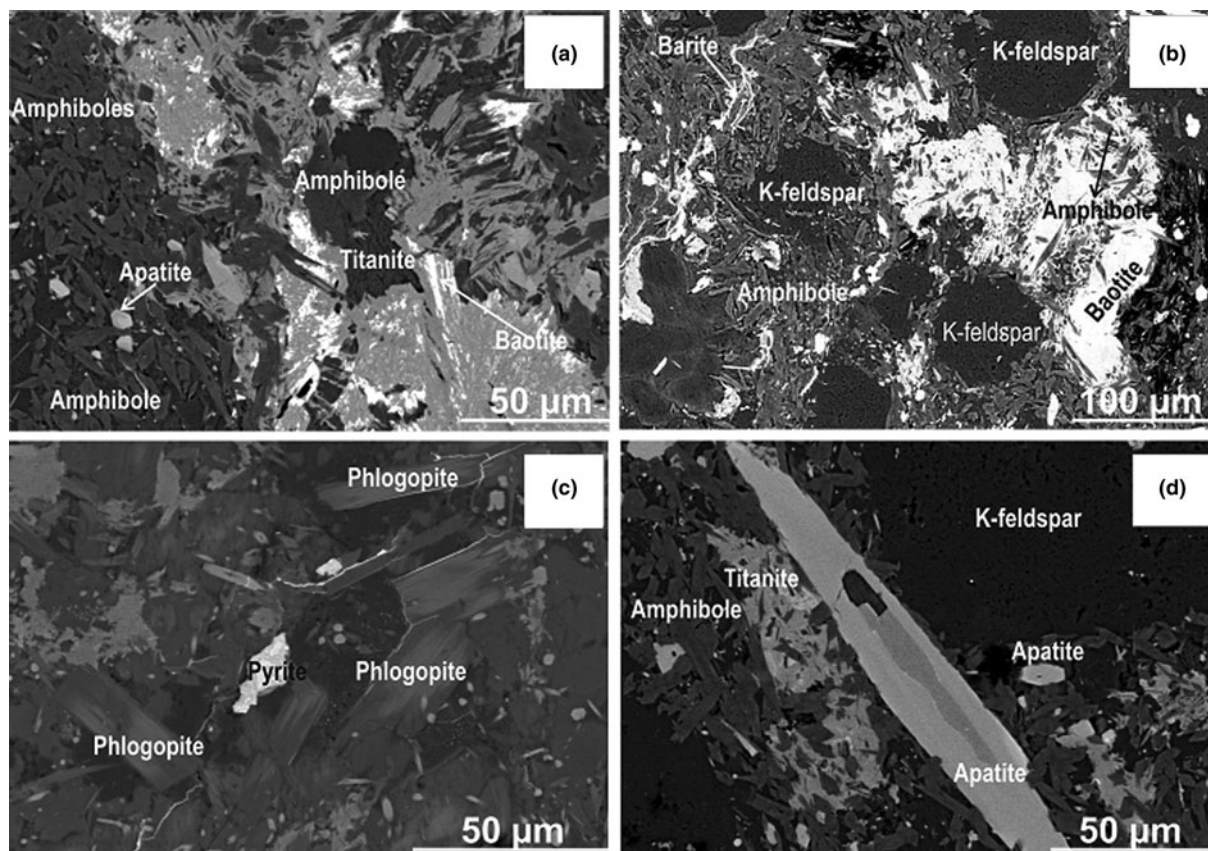
**Fig. 6.** Back-scatter electron images of: (*a*) wedge-shaped amphibole, titanite and baotite together with euhedral apatite represent the groundmass material; (*b*) baotite in association with amphiboles, with potassium feldspar pseudomorphs, groundmass amphiboles and a fine-grained baryte veinlet also visible; (*c*) ground-mass phlogopites in the Gundrapalli lamproite; and (*d*) elongated zoned apatite together with amphibole and potassium feldspar.

**Table 1.** Representative compositions (wt.%) and calculated mineral formula (in apfu) for Gundrapalli amphiboles.

| | K-rct GL1 | K-rct GL2 | K-rct GL3 | K-rct GL4 | K-rct GL5 | K-arf GL6 | Mg-rbk GL7 | K-rct GL8 | K-rct GL9 | K-rct GL10 | Ti-rich K-Mg-arf GL 11 light | K-Mg-arf GL 11 dark | ktp GL 12 light | K-Mg-arf GL 12 dark | K-ferri-ktp GL13 |
|---|---|---|---|---|---|---|---|---|---|---|---|---|---|---|---|
| **Wt.%** | | | | | | | | | | | | | | | |
| $SiO_2$ | 54.18 | 53.38 | 53.60 | 53.60 | 53.09 | 54.02 | 55.45 | 53.47 | 53.17 | 54.63 | 53.77 | 53.94 | 52.31 | 54.06 | 52.30 |
| $TiO_2$ | 2.68 | 0.70 | 1.82 | 1.23 | 2.97 | 2.41 | 1.76 | 2.53 | 2.17 | 1.71 | 4.97 | 4.69 | 9.04 | 1.86 | 1.58 |
| $Al_2O_3$ | 0.18 | n.d. | n.d. | n.d. | n.d. | n.d. | 0.24 | 0.28 | 0.19 | n.d. | 0.42 | n.d. | 0.27 | n.d. | n.d. |
| FeO* | 10.19 | 17.88 | 15.90 | 15.32 | 16.52 | 20.20 | 18.84 | 14.19 | 16.71 | 13.50 | 14.64 | 8.64 | 14.11 | 10.50 | 17.51 |
| MnO | 0.19 | 0.34 | n.d. | 0.31 | 0.25 | 0.36 | n.d. | 0.24 | 0.27 | n.d. | n.d. | n.d. | n.d. | 0.36 | n.d. |
| MgO | 16.71 | 11.77 | 12.99 | 13.36 | 12.09 | 9.25 | 10.61 | 13.45 | 11.99 | 15.39 | 13.54 | 16.70 | 11.30 | 17.15 | 12.56 |
| CaO | 5.60 | 4.32 | 4.53 | 4.76 | 4.67 | 0.62 | 0.48 | 4.69 | 4.36 | 5.18 | 2.06 | 3.12 | 5.32 | 2.97 | 4.31 |
| $Na_2O$ | 3.87 | 4.50 | 4.45 | 4.12 | 4.34 | 6.66 | 6.62 | 4.27 | 4.33 | 4.19 | 6.50 | 6.02 | 6.22 | 5.60 | 5.30 |
| $K_2O$ | 5.37 | 5.22 | 5.23 | 5.20 | 5.15 | 5.18 | 2.36 | 5.17 | 5.27 | 5.42 | 3.26 | 4.80 | 2.25 | 5.55 | 5.21 |
| F | 1.20 | n.d. | 0.82 | 0.85 | 0.54 | n.d. | n.d. | 0.73 | 0.46 | 0.75 | n.d. | n.d. | n.d. | n.d. | n.d. |
| Total | 98.97 | 98.11 | 98.52 | 97.90 | 99.08 | 98.70 | 96.36 | 98.29 | 98.46 | 100.02 | 99.16 | 97.91 | 100.82 | 98.05 | 98.77 |
| **Atoms per formula unit calculated on the basis of 23 atoms of oxygen** | | | | | | | | | | | | | | | |
| Si | 7.719 | 8.004 | 7.948 | 7.982 | 7.868 | 8.071 | 8.133 | 7.892 | 7.928 | 7.893 | 7.769 | 7.788 | 7.496 | 7.786 | 7.72 |
| Ti | 0.251 | – | 0.052 | 0.018 | 0.132 | – | – | 0.059 | 0.038 | 0.107 | 0.159 | 0.212 | 0.459 | 0.202 | 0.175 |
| Al | 0.030 | – | – | – | – | – | – | 0.049 | 0.033 | – | 0.072 | n.d. | 0.046 | – | – |
| Fe | 1.393 | 2.101 | 1.972 | 1.908 | 2.048 | 2.266 | 1.483 | 1.752 | 2.084 | 1.590 | 1.586 | 1.043 | 1.691 | 0.695 | 1.454 |
| Mn | – | 0.043 | – | 0.007 | 0.031 | 0.046 | – | 0.030 | 0.034 | – | – | – | – | 0.044 | – |
| Mg | 3.549 | 2.631 | 2.872 | 2.966 | 2.671 | 2.060 | 2.320 | 2.960 | 2.665 | 3.315 | 2.917 | 3.595 | 2.414 | 3.682 | 2.764 |
| Ca | 0.855 | 0.694 | 0.720 | 0.759 | 0.742 | 0.099 | 0.075 | 0.742 | 0.697 | 0.802 | 0.319 | 0.483 | 0.817 | 0.458 | 0.682 |
| Na | 1.055 | 1.306 | 1.279 | 1.190 | 1.247 | 1.901 | 1.883 | 1.222 | 1.252 | 1.173 | 1.615 | 1.517 | 1.183 | 1.542 | 1.318 |
| K | 0.976 | 0.999 | 0.989 | 0.988 | 0.974 | 0.987 | 0.442 | 0.974 | 1.002 | 0.999 | 0.601 | 0.884 | 0.411 | 1.02 | 0.981 |
| F | 0.395 | – | 0.385 | 0.400 | 0.253 | – | – | 0.341 | 0.217 | 0.343 | – | – | – | – | – |

n.d. – not detected; K – potassic; Mg – magnesio; rct – richterite; arf – arfvedsonite; ktp – katophorite

FeO* – total Fe expressed as FeO; 11, 12 are zoned and associated with baotite.

**Table 2.** Representative compositions (wt.%) and calculated mineral formulae (in apfu) for Gundrapalli K-feldspars.

|  | GL1 | GL2 | GL3 | GL4 | GL5 | GL6 | GL7 | GL8 | GL9 |
|---|---|---|---|---|---|---|---|---|---|
| Wt.% |  |  |  |  |  |  |  |  |  |
| $SiO_2$ | 64.80 | 64.49 | 64.60 | 65.42 | 63.85 | 63.98 | 63.87 | 63.97 | 63.96 |
| $Al_2O_3$ | 17.77 | 18.39 | 18.18 | 18.53 | 17.91 | 17.75 | 18.31 | 18.17 | 18.25 |
| FeO* | 0.53 | 0.38 | 0.62 | 0.27 | 0.60 | 0.46 | n.d. | 0.31 | n.d. |
| $Na_2O$ | 0.22 | n.d. | n.d. | n.d. | n.d. | 0.21 | n.d. | 0.24 | n.d. |
| $K_2O$ | 16.26 | 16.23 | 15.97 | 16.45 | 16.68 | 17.17 | 17.43 | 17.41 | 17.20 |
| Total | 99.58 | 99.49 | 99.37 | 100.67 | 99.04 | 99.57 | 99.61 | 100.10 | 99.41 |
| Atoms per formula unit calculated on the basis of 8 atoms of oxygen |  |  |  |  |  |  |  |  |  |
| Si | 3.013 | 2.997 | 3.004 | 3.002 | 2.996 | 2.995 | 2.984 | 2.981 | 2.990 |
| Al | 0.974 | 1.007 | 0.996 | 1.002 | 0.990 | 0.979 | 1.008 | 0.998 | 1.005 |
| Fe | 0.021 | 0.015 | 0.024 | 0.010 | 0.024 | 0.018 | – | 0.012 | – |
| Na | 0.020 | – | – | – | – | 0.019 | – | 0.022 | – |
| K | 0.965 | 0.962 | 0.947 | 0.963 | 0.998 | 1.025 | 1.039 | 1.035 | 1.026 |

n.d. – not detected
FeO* – total Fe expressed as FeO

**Table 3.** Representative compositions (wt.%) and calculated mineral formulae (in apfu) for Gundrapalli phlogopites.

|  | GL1 | GL2 | GL3 | GL4 | GL5 | GL6 |
|---|---|---|---|---|---|---|
| Wt.% |  |  |  |  |  |  |
| $SiO_2$ | 37.39 | 38.61 | 38.94 | 38.09 | 39.96 | 39.99 |
| $TiO_2$ | 4.96 | 4.14 | 5.18 | 4.82 | 5.99 | 5.86 |
| $Al_2O_3$ | 7.1 | 8.66 | 6.93 | 5.99 | 5.64 | 5.54 |
| FeO* | 19.91 | 19.61 | 18.52 | 18.71 | 19.09 | 17.63 |
| MgO | 14.32 | 15.65 | 15.34 | 14.28 | 14.55 | 15.81 |
| $K_2O$ | 8.73 | 8.44 | 8.15 | 8.94 | 9.58 | 8.98 |
| BaO | 1.60 | 1.31 | 1.58 | 1.48 | 1.36 | 1.82 |
| F | 1.11 | 1.12 | 1.35 | 1.49 | 1.45 | 1.83 |
| Total | 94.01 | 96.42 | 94.64 | 92.31 | 96.17 | 95.63 |
| Atoms per formula unit calculated on the basis of 16 cations |  |  |  |  |  |  |
| Si | 6.028 | 6.001 | 6.207 | 6.238 | 6.298 | 6.310 |
| Ti | 0.601 | 0.484 | 0.621 | 0.594 | 0.710 | 0.695 |
| Al | 1.349 | 1.586 | 1.302 | 1.156 | 1.048 | 1.030 |
| Fe | 2.684 | 2.549 | 2.469 | 2.563 | 2.516 | 2.326 |
| Mg | 3.441 | 3.626 | 3.645 | 3.486 | 3.418 | 3.719 |
| K | 1.795 | 1.674 | 1.657 | 1.868 | 1.926 | 1.808 |
| Ba | 0.101 | 0.080 | 0.099 | 0.095 | 0.084 | 0.113 |
| F | 0.566 | 0.551 | 0.681 | 0.772 | 0.723 | 0.913 |

n.d. – not detected
FeO* – total Fe expressed as FeO

**Table 4.** Representative compositions (wt.%) and calculated mineral formulae (in apfu) for Gundrapalli pyroxenes.

|  | GL1 | GL2 | GL3 | GL4 | GL5 | GL6 |
|---|---|---|---|---|---|---|
| Wt.% |  |  |  |  |  |  |
| $SiO_2$ | 50.31 | 49.40 | 51.20 | 51.68 | 52.07 | 51.28 |
| $TiO_2$ | 2.84 | 4.10 | 3.89 | 2.99 | 2.81 | 3.35 |
| $Al_2O_3$ | 0.76 | 0.71 | 0.69 | 0.66 | 0.74 | 0.77 |
| FeO* | 5.38 | 5.24 | 5.15 | 4.89 | 4.97 | 5.23 |
| MgO | 16.73 | 16.36 | 16.79 | 16.66 | 17.09 | 17.13 |
| CaO | 22.29 | 23.18 | 22.3 | 21.9 | 22.51 | 22.06 |
| $Na_2O$ | 0.53 | 0.65 | 0.75 | 0.67 | 0.77 | 0.68 |
| Total | 98.84 | 99.64 | 100.77 | 99.45 | 100.96 | 100.50 |
| Atoms per formula unit calculated on the basis of 4 cations |  |  |  |  |  |  |
| Si | 1.869 | 1.826 | 1.868 | 1.907 | 1.888 | 1.872 |
| Ti | 0.079 | 0.114 | 0.107 | 0.083 | 0.077 | 0.092 |
| Al | 0.033 | 0.031 | 0.030 | 0.029 | 0.032 | 0.033 |
| Fe | 0.167 | 0.162 | 0.157 | 0.151 | 0.151 | 0.160 |
| Mg | 0.926 | 0.902 | 0.913 | 0.917 | 0.924 | 0.932 |
| Ca | 0.887 | 0.918 | 0.872 | 0.866 | 0.875 | 0.863 |
| Na | 0.038 | 0.047 | 0.053 | 0.048 | 0.054 | 0.048 |

n.d. – not detected
FeO* – total Fe expressed as FeO

lamproites and carbonatites as a result of auto-metasomatism in these rocks through fluids (Kullerud *et al.*, 2012 and references therein). The baotites from different provenances such as pegmatites, fenitised granites, hydrothermal quartz veins, metasomatites, volcaniclastic breccia etc. demonstrate the intense effects of late-to-post-magmatic processes involving fluids enriched in chlorine and fluorine.

The presence of baotite in the Gundrapalli dyke is the first report of baotite from a lamproite in India. Baotite compositions given in Table 6 have been recalculated on the basis of 16 cations, with the resulting structural formula being close to the ideal Ti-rich end-member $Ba_4Ti_8Si_4O_{28}Cl$. Representative compositions indicate (40.71–37.89 wt.%) BaO, (40.52–39.32 wt.%) $TiO_2$, (1.28–0.82 wt.%) $Nb_2O_5$ and 2.24–1.97 wt.% Cl. Minor amounts of Ca have substituted for Ba and some minor Nb and Fe have substituted for Ti (Table 6).

We have tried to interpret the coupled element exchange mechanisms in the Gundrapalli baotite following Copper (1996) and Kullerud *et al.* (2012). The binary Ti–Nb, Ti–Fe, Ti–Ba and Ti–Cl plots of baotites of Gundrapalli lamproites and baotites

reported from different alkaline/peralkaline rock types from various global localities are given in Fig. 7 (Supplementary Table S1). In the Ti–Nb diagram the Gundrapalli baotites plot close to the slope –⅔ as is the case for Kvaløya and SW Bohemia (Copper, 1996; Kullerud *et al.*, 2012; Krmíček *et al.*, 2011). In the Ti–Fe diagram the data plot close to a line with a slope –⅓. These observations support a coupled Ti–Nb exchange mechanism in baotite in the form of $3Ti^{4+} = 2Nb^{5+} + Fe^{2+}$, as suggested by Cooper (1996) and Kullerud *et al.* (2012). All Gundrapalli baotites cluster near the $Ba_4Ti_8Si_4O_{28}Cl$ end-member together with Kvaløya and SW Bohemia baotites along the tie line between the Nb-rich end-member $Ba_4Ti_2Fe_2^{2+}Nb_4Si_4O_{28}Cl$ and Nb-free end-member $Ba_4Ti_8Si_4O_{28}Cl$ [Fig. 7; Supplementary Table S1; Cooper (1996); Kullerud *et al.* (2012)].

The role of Cl in baotite is insignificant to balance the structure of the mineral electrostatically (Potter and Mitchell, 2005; Kullerud *et al.*, 2012 and references therein). The chlorine contents in baotites have a restricted range varying between 1.3 wt.% to 3.1 wt.% (Nemec 1987; Potter and Mitchell 2005; Kullerud *et al.*, 2012 and references therein). Chakhmouradian and Mitchell (2002) reported the formation of baotite together with other fluorine-rich minerals such as *REE* fluorocarbonates,

**Table 5.** Representative compositions (wt.%) of Gundrapalli and Kvaløya apatites.

| | 1 | 2 | 3 | 4 | 5 | 6 | 7 |
|---|---|---|---|---|---|---|---|
| | 1 | 2 | 3 | 4 | 5C | 5R | 6C |
| $P_2O_5$ | 41.59 | 42.85 | 40.21 | 39.87 | 42.16 | 40.03 | 39.9 |
| $SiO_2$ | 3.03 | 1.40 | 1.51 | 1.21 | 0.37 | 1.14 | 1.80 |
| FeO* | 0.66 | 0.47 | 0.32 | 0.39 | n.d. | n.d. | 0.37 |
| CaO | 49.01 | 48.51 | 51.53 | 51.64 | 54.95 | 52.63 | 51.15 |
| SrO | 3.21 | 3.22 | 3.17 | 3.59 | 0.68 | 3.18 | 3.44 |
| BaO | n.d. | n.d. | 0.74 | 0.31 | n.d. | n.d. | n.d. |
| $Na_2O$ | n.d. | n.d. | n.d. | n.d. | 0.32 | n.d. | n.d. |
| $La_2O_3$ | n.d. | 0.40 | n.d. | 0.32 | n.d. | n.d. | 0.44 |
| $Ce_2O_3$ | 1.04 | 1.12 | n.d. | 0.95 | n.d. | 0.99 | 1.43 |
| $Nd_2O_3$ | n.d. | 0.41 | n.d. | 0.31 | n.d. | n.d. | 0.56 |
| F | 2.49 | 3.48 | 3.77 | 3.12 | 2.44 | 3.25 | 3.05 |
| Total | 98.54 | 98.38 | 97.48 | 98.59 | 98.48 | 97.97 | 99.09 |

| | 8 | 9 | 10 | 11 | 12 | 13 | 14 |
|---|---|---|---|---|---|---|---|
| | 6R | C | R | C | R | C | R |
| $P_2O_5$ | 39.16 | 40.76 | 40.40 | 41.94 | 38.03 | 41.17 | 40.20 |
| $SiO_2$ | 1.29 | 0.18 | 0.13 | 0.19 | 0.04 | 0.22 | 0.26 |
| FeO* | 0.33 | 0.13 | 0.19 | 0.18 | n.d. | 0.12 | 0.12 |
| CaO | 48.93 | 50.06 | 39.78 | 54.62 | 42.54 | 52.30 | 48.88 |
| SrO | 6.20 | 3.54 | 8.89 | 0.18 | 8.54 | 2.67 | 5.04 |
| BaO | n.d. | 0.37 | 0.12 | n.d. | 0.13 | 0.22 | 0.66 |
| $Na_2O$ | n.d. | 0.12 | 1.60 | 0.09 | 1.47 | 0.06 | 0.25 |
| $La_2O_3$ | 0.50 | 0.25 | 1.17 | 0.13 | 1.52 | 0.17 | 0.44 |
| $Ce_2O_3$ | 1.71 | 0.64 | 3.59 | 0.35 | 3.71 | 0.46 | 1.07 |
| $Nd_2O_3$ | 0.50 | 0.29 | 1.80 | 0.19 | 1.43 | 0.22 | 0.46 |
| F | 3.12 | 3.25 | 3.25 | 4.50 | 2.79 | 3.05 | 3.27 |
| Total | 98.62 | 96.34 | 97.67 | 97.87 | 97.41 | 97.61 | 97.38 |

n.d. – not detected; C – Core; R – Rim; 1–8: Gundrapalli apatites; 9–14: Kvaloya apatites
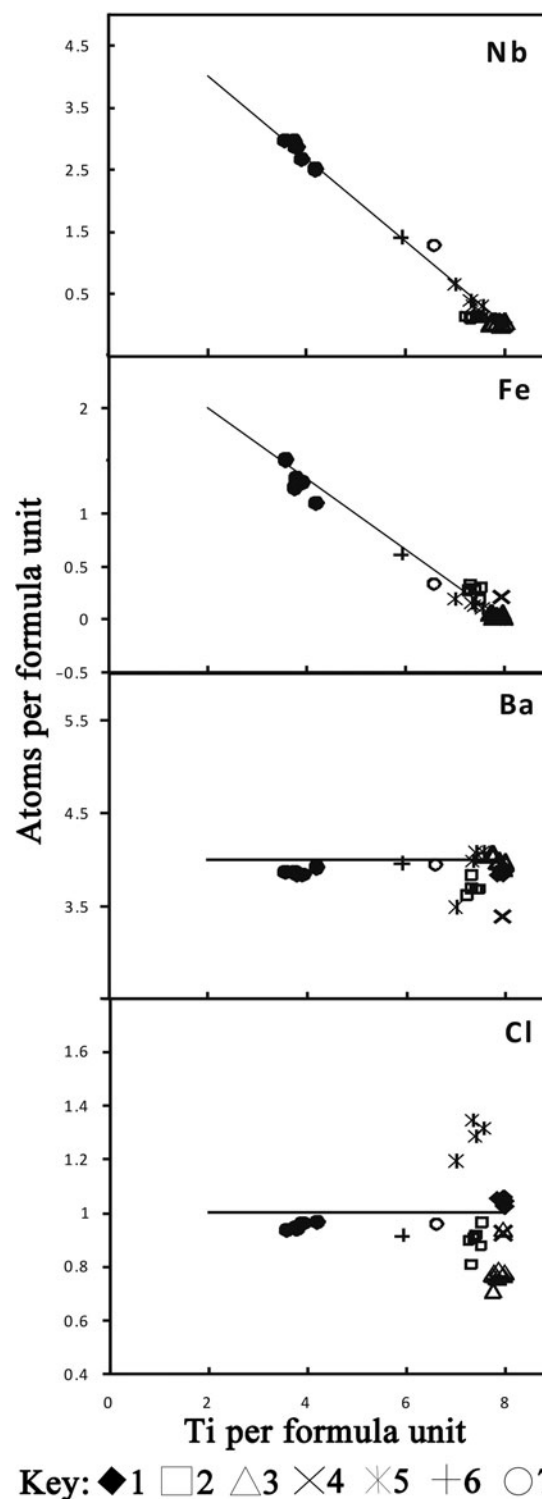FeO* – total Fe expressed as FeO

**Table 6.** Representative compositions (wt.%) and calculated mineral formulae (in apfu) for Gundrapalli and Kvaløya baotites.

| | 1 | 2 | 3 | 4 | 5 | 6 | 7** | S.D. |
|---|---|---|---|---|---|---|---|---|
| Wt.% | | | | | | | | |
| $SiO_2$ | 15.86 | 15.87 | 15.26 | 15.52 | 15.90 | 15.92 | 15.70 | 0.21 |
| $TiO_2$ | 40.52 | 39.87 | 39.56 | 39.77 | 40.09 | 39.32 | 41.91 | 0.23 |
| $Al_2O_3$ | n.d. | n.d. | n.d. | n.d. | n.d. | n.d. | 0.32 | 0.03 |
| FeO* | 0.88 | 1.38 | 1.33 | 1.41 | 1.38 | 1.65 | n.d. | |
| CaO | 2.30 | 2.12 | 3.02 | 0.40 | 2.93 | 1.65 | 0.06 | 0.09 |
| BaO | 38.34 | 38.11 | 37.89 | 40.71 | 38.71 | 39.40 | 39.20 | 0.24 |
| SrO | n.d. | n.d. | n.d. | n.d. | n.d. | n.d. | 0.17 | 0.05 |
| $K_2O$ | n.d. | n.d. | n.d. | n.d. | n.d. | n.d. | 0.16 | 0.07 |
| $Nb_2O_5$ | 1.20 | 1.25 | 1.28 | 1.01 | 0.82 | 1.10 | 0.35 | 0.17 |
| Cl | 2.11 | 2.20 | 2.19 | 2.24 | 1.97 | 2.17 | 2.43 | |
| Total | 101.21 | 100.80 | 100.53 | 101.06 | 101.80 | 101.21 | 100.30 | |
| O = Cl | 0.48 | 0.50 | 0.49 | 0.51 | 0.44 | 0.49 | 0.55 | |
| Total | 100.73 | 100.30 | 100.04 | 100.55 | 101.36 | 100.72 | 99.75 | |
| Atoms per formula unit calculated on the basis of 16 cations | | | | | | | | |
| Si | 3.90 | 3.92 | 3.95 | 3.91 | 3.86 | 3.94 | 3.96 | |
| Ti | 7.49 | 7.41 | 7.24 | 7.54 | 7.32 | 7.33 | 7.94 | |
| Al | – | – | – | – | – | – | 0.10 | |
| Fe | 0.18 | 0.29 | 0.27 | 0.30 | 0.28 | 0.34 | – | |
| Ca | 0.61 | 0.56 | 0.79 | 0.11 | 0.76 | 0.44 | 0.02 | |
| Ba | 3.69 | 3.69 | 3.61 | 4.02 | 3.68 | 3.83 | 3.87 | |
| Sr | – | – | – | – | – | – | 0.02 | |
| K | – | – | – | – | – | – | 0.05 | |
| Nb | 0.13 | 0.14 | 0.14 | 0.12 | 0.09 | 0.12 | 0.04 | |
| Cl | 0.88 | 0.92 | 0.90 | 0.96 | 0.81 | 0.91 | 1.04 | |

n.d. – not detected; FeO* – total Fe expressed as FeO; S.D. – standard deviation
** #7 = average of Kvaløya lamproite from Norway, n = 38



**Fig. 7.** Binary Nb–Ti, Fe–Ti, Ba–Ti and Cl–Ti plots for baotites of Gundrapalli lamproite and other world-wide localities. Key: 1 – Kvaløya, Norway (Kullerud *et al.*, 2012); 2 – Gundrapalli, India (present work); 3 – Variscan, Bohemia, Czech Republic (Nemec, 1987; Krmíček et al., 2011); 4 – Montana, USA (Chakhmouradian and Mitchell, 2002); 5 – Ontario, Canada (Potter and Mitchell, 2005); 6 – Bayan-Obo, Mongolia, China (Peng, 1959); 7 – Bayan-Obo, Mongolia, China (Semenov et al., 1961); 8 – Haast River, New Zealand (Cooper, 1996).

calcite and fluorapatite from alkaline pegmatites in the presence of high-F fluids. Similarly, Krmíček et al. (2011) and Kullerud et al. (2012) reported late-magmatic crystallisation of baotite together with Sr-rich fluorapatite from lamproite-like dykes in SW Bohemia, Czech Republic and the Kvaløya lamproite, Norway, respectively. These workers inferred that the Cl-rich

**Table 7.** Global occurrence of baotites from alkaline and associated rocks (modified after Kullerud et al., 2012).

| No | Rock type | Locality | Compositional variation | References |
|---|---|---|---|---|
| 1 | Hydrothermal quartz vein | Bayan-Obo, Mongolia, China | $Ba_4Ti_4(Ti_2Nb_{1.4}Fe_{0.6})ClO_{16}Si_4O_{12}$<br>$Ba_4Ti_7NbSi_4O_{28}Cl$ | Peng (1959)<br>Semenov et al. (1961) |
| 2 | Carbonatites and carbonatite veins and dykes | Ravalli County, Montana, USA<br>Beriah, Buryatia, Russia<br>Lueshe, Democratic Republic of Congo<br>Haast River, New Zealand | $Ba_4Ti_3(Nb,Fe)_5Si_4O_{28}Cl$ | Henrich et al. (1962)<br>Koneva et al. (2008)<br>Wall et al. (1996)<br>Cooper (1996) |
| 3 | Alkali-granite pegmatites and hydrothermal rocks | Zagi, Pakistan<br>Dara-i-Pioz, Tajikistan | | Obodda and Leavens (2004)<br>Karpenko and Pautov (2002) |
| | Alkaline pegmatites<br>Fenitised granite | Gordon Butte, Montana, USA<br>Kvaløya, Norway | $Ba_4,Ti_4(Ti,Nb,Fe)_4(Si_4O_{12})O_{16}Cl$<br>$Ba_4Ti_8Si_4O_{28}Cl$ | Chakhmouradian and Mitchell (2002)<br>Kullerud et al. (2012) |
| 4 | Lamproite-like dykes | SW Bohemia, Czech Republic | $Ba_4Ti_8Si_4O_{28}Cl_{0.6-1}$<br>$Ba_4Ti_8Si_4O_{28}Cl$ | Nemec (1987)<br>Krmíček et al. (2011) |
| 5 | Lamproite | Kostomuksha, Karelia, Russia<br>Kvaløya, Norway | $Ba_4Ti_8Si_4O_{28}Cl$ | Rudashevsky et al. (2011)<br>Kullerud et al. (2012) |
| 6 | Natrolite veins | Khibinsk mountains, Kola, Russia<br>San Benito, California, USA | | Pekov et al. (2000)<br>Wise and Gill (1977) |
| 7 | Alkaline metasomatites | Western Urals<br>Primorye, Russia | $Ba_6(Ti_4Nb)_2O_{22}Si_4O_{12}Cl$ | Efimov and Es'kova (1973)<br>Shuriga et al. (1980) |
| | Altered volcaniclastic breccia | Ontario, Canada | $Ba_4(Ti,Nb)_8Si_4O_{28}Cl$ | Potter and Mitchell (2005) |
| 8 | Hydrothermal veins in calcareous siltstones | Pyrenees, France | | Johan et al. (1991) |
| 9 | Lamproite | Gundrapalli, Telengana, India | $Ba_4Ti_8Si_4O_{28}Cl$ | Gurmeet Kaur and Mitchell (2017) |

and F-devoid baotite and F-rich minerals such as fluorapatite, fluorocarbonates, F-rich silicates and calcite can form in equilibrium with a late-stage fluid enriched in F, $CO_2$ and Cl.

Chlorine-bearing minerals are rare in nature due to the strong preference of Cl for late-stage fluids (Kullerud et al., 2012 and references therein). The silicates, i.e. amphiboles and micas (phlogopites, biotites), commonly incorporate fluorine when fluids are enriched both in fluorine and chlorine, whereas they incorporate chlorine if the fluids are enriched in chlorine and poor in fluorine (Kullerud, 1995, 1996). The silicate mineral baotite is unique in the sense that it extracts chlorine instead of fluorine from fluids enriched both in fluorine and chlorine (Kullerud et al., 2012 and references therein).

## Mineralogy of Gundrapalli vis-à-vis Kvaløya lamproite

The Kvaløya lamproite dyke is intrusive into Paleoproterozoic granite, part of the West Troms Basement Complex, on the island Kvaløya, northern Norway (Kullerud et al., 2011; Kullerud et al., 2012 and references therein). The Gundrapalli lamproite dyke is also intrusive into granite of Peninsular Gneissic Complex, Eastern Dharwar Craton (Fig. 2). The Kvaløya lamproite contains fluorapatite, phlogopite (enriched in fluorine) and Cl-enriched baotite similar to that of the Gundrapalli lamproite, as discussed above. The major similarity between the two rocks is the presence of zoned, phenocrystal-to-microphenocrystal apatite. The Kvaløya zoned apatites are typically impoverished in SrO in the core and are enriched in SrO at their rims and are quite similar to the Gundrapalli phenocrystal-to-microphenocrystal apatites. The Kvaløya and Gundrapalli apatites are enriched in fluorine (Table 5). There is a striking similarity between the baotite found at Kvaløya and Gundrapalli in that in both it forms aggregates with radiating structures instead of well-defined crystals and is associated closely with rutile, amphiboles and also titanite (at Gundrapalli). Baotites from both the Norwegian and Indian lamproites are almost Nb-free types with the composition $Ba_4Ti_8Si_4O_{28}Cl$ (Table 6). The Kvaløya lamproite contains phlogopite and apatite enriched in

fluorine and baotite enriched in chlorine analogous to apatite, phlogopite and baotite of the Gundrapalli lamproite.

## Discussion and conclusions

Alkaline/peralkaline magmatism is prevalent in the eastern Dharwar craton of southern India. Numerous new occurrences of lamproite dykes from, and around, the Palaeoproterozoic–Mesoproterozoic Cuddapah Basin provides an opportunity to comprehend the nature of the subcontinental lithospheric mantle in southern India. The mineralogy of a newly discovered dyke at Gundrapalli village in the Ramadugu lamproite field reveals the nature of the parental magma which was responsible for the observed mineral paragenesis: katophorite and potassic-ferri-katophorite; Al-poor pyroxene; phlogopite; K-feldspars (leucite); spinel (chromite-magnesiochromite); apatite (Sr and fluorine-rich), titanite; rutile; calcite; baryte; and baotite. The absence of Ba-Ti-Zr minerals, such as wadeite and priderite from the Gundrapalli dyke have been compensated for by the presence of baotite, rutile, baryte and hydro-zircons. The presence of secondary phases such as allanite, hydro-zircon, chlorite, quartz and cryptocrystalline $SiO_2$, implies that the dyke has undergone varied degrees of deuteric alteration. On the basis of its typomorphic major mineralogy the Gundrapalli dyke is classified as a pseudoleucite-phlogopite-amphibole-lamproite. The presence of baotite in the Gundrapalli dyke (first occurrence reported from India) is similar to the baotite paragenesis from the Kvaløya lamproite dyke in Norway. The high Cl-content of baotite in Gundrapalli, as is also the case at Kvaløya, indicates partitioning of Cl into baotite in the Cl-bearing F-rich hydrous fluid (Kullerud et al., 2012 and references therein). From the investigations of the Kvaløya lamproite we deduce that the Gundrapalli baotite also formed as a late-stage mineral from a fluorine- and chlorine-enriched fluid phase of the lamproite magma. The presence of the Ti- and Ba-rich phases baotite, rutile, baryte, allanite and titanite suggest high $a_{Ti}$, $a_{Ba}$, in equilibrium with high F-, Cl-bearing hydrous fluids operational during the formation of Gundrapalli lamproite.

In summary: (1) the Gundrapalli dyke is a pseudoleucite-phlogopite-amphibole lamproite; (2) the typomorphic Ba-Ti-Zr minerals of lamproites in the Gundrapalli lamproite dyke are represented by baotite, rutile, baryte and hydro-zircons; (3) baotite has been identified for the first time from an Indian lamproite; (4) the secondary phases allanite, chlorite, quartz and cryptocrystalline silica, implies deuteric alteration of the Gundrapalli lamproite dyke; (5) the Gundrapalli lamproite mineralogy is comparable with Kvaløya lamproite (Norway); and (6) the presence of the Ti- and Ba- rich phases baotite, rutile, baryte, allanite and titanite suggest high $a_{Ti}$, $a_{Ba}$ in equilibrium with F- and Cl-bearing hydrous fluids.

# References

Ahmed S. and Kumar A. (2012) *Search for Kimberlite/lamproite in Paluvayi Block in Nalgonda District, Andhra Pradesh.* Geological Survey of India Report. Kolkotta, India. www.portal.gsi.gov.in.

Chakhmouradian A.C. and Mitchell R.H. (2002) The mineralogy of Ba- and Zr-rich alkaline pegmatites from Gordon Butte, Crazy Mountains (Montana, USA): comparisons between potassic and sodic agpaitic pegmatites. *Contributions to Mineralogy and Petrology*, **143**, 93–114.

Chalapathi Rao N.V., Gibson S.A., Pyle D.M. and Dickin A.P. (2004) Petrogenesis of Proterozoic lamproites and kimberlites from the Cuddapah Basin and Dharwar craton, southern India, *Journal of Petrology*, **45**(5), 907–948.

Chalapathi Rao N.V., Kamde G., Kale H.G. and Dongre A. (2010) Mesoproterozoic lamproites from the Krishna Valley, Eastern Dharwar craton, southern India: petrogenesis and diamond prospectivity. *Precambrian Research*, **177**, 103–130.

Chalapathi-Rao N.V., Wu F.Y., Mitchell R.H., Li Q.L. and Lehmann B. (2013) Mesoproterozoic U-Pb ages, trace element and Sr-Nd isotopic composition of perovskite from kimberlites of the Eastern Dharwar craton, southern India: Distinct mantle sources and a widespread 1.1 Ga tectonomagmatic event. *Chemical Geology*, **353**, 48–64.

Chalapathi Rao N.V., Kumar A., Sahoo S., Dongre A. N. and Talukdar D. (2014) Petrology and petrogenesis of Mesoproterozoic lamproites from the Ramadugu field, NW margin of the Cuddapah basin, Eastern Dharwar craton, southern India. *Lithos*, **196–197**, 150–168.

Chalapathi Rao N.V., Atiullah, Kumar A., Sahoo S., Nanda P., Chahong N., Lehmann B. and Rao K.V.S. (2016) Petrogenesis of Mesoproterozoic lamproite dykes from the Garledinne (Banganapalle) cluster, south-western Cuddapah Basin, southern India. *Mineralogy and Petrology*, **110**, 247–268.

Cooper A.F. (1996) Nb-rich baotite in carbonatites and fenites at Haast River, New Zealand. *Mineralogical Magazine*, **60**, 473–482.

Davies G.R., Stolz A.J., Mahotkin I.L., Nowell G.M. and Pearson D.G. (2006) Trace element and Sr–Pb–Nd–Hf isotope evidence for ancient, fluid-dominated enrichment of the source of Aladan shield lamproites. *Journal of Petrology*, **47**, 1119–1146.

Fareeduddin and Mitchell R.H. (2012) *Diamonds and their Source Rocks in India.* Geological Society of India, Bangalore, India, 434 pp.

Fritschle T., Prelević D., Foley S.F. and Jacob D.E. (2013) Petrological characterization of the mantle source of Mediterranean lamproites: Indications

from major and trace elements of phlogopite. *Chemical Geology*, **353**, 267–279.

Gurmeet Kaur and Mitchell R.H. (2013) Mineralogy of the P2-West 'Kimberlite', Wajrakarur kimberlite field, Andhra Pradesh, India: kimberlite or lamproite? *Mineralogical Magazine*, **77**, 3175–3196.

Gurmeet Kaur and Mitchell R.H. (2016) Mineralogy of the P-12 K-Ti-richterite diopside olivine lamproite from Wajrakarur, Andhra Pradesh, India: implications for subduction-related magmatism in eastern India. *Mineralogy and Petrology*, **110**, 223–245.

Gurmeet Kaur and Mitchell R.H. (2017) Mineralogy of the baotite-bearing Gundrapalli lamproite, Nalgonda district, Telangana, India. 11th *International Kimberlite Conference.* Extended abstract 4499, 1–3.

Gurmeet Kaur, Korakoppa M., Fareeduddin and Pruseth K.L. (2013) Petrology of P-5 and P-13 "kimberlites" from Lattavaram kimberlite cluster, Wajrakarur Kimberlite Field, Andhra Pradesh, India: Reclassification as lamproites. Pp 183–194 in: *Proceedings of the Xth International Kimberlite Conference* (D.G. Pearson, H.S. Grutter, J.W. Harris, B.A. Kjarsgaard, H. O'brien, N.V. Chalapathi Rao and R.S.J. Sparks, editors). Geological Society of India, Springer Publication.

Gurmeet Kaur, Mitchell R.H. and Ahmed S. (2016) Typomorphic mineralogy of the Vattikod lamproites from Mesoproterozoic Ramadugu Lamproite Field, Nalgonda District, Telangana, India: A plausible manifestation of subduction-related alkaline magmatism in the Eastern Ghats Mobile Belt? *35th International Geological Congress, South Africa Meeting.* Abstract #3482. Available at https://www.americangeosciences.org/sites/default/files/igc/5423.pdf

Gurmeet Kaur, Mitchell R.H. and Ahmed S. (2018) Mineralogy of the Vattikod lamproite dykes, Ramadugu Lamproite Field, Nalgonda District, Telangana: A possible expression of ancient subduction-related alkaline magmatism along Eastern Ghats Mobile Belt, India. *Mineralogical Magazine*, **82**(1), 35–58.

Heinrich E.W., Boyer W.H. and Crowley F.A. (1962) Baotite from Ravalli County, Montana. *American Mineralogist*, **47**, 987–993.

Karpenko V. and Pautov L. (2002) Formation of baotite in alkaline rocks of a moraine of Dara-i-Pioz Glacier, Tadjikistan. *Neues Jahrbuch Mineral Monatshefte*, **10**, 459–467.

Koneva A.A., Konev A.A. and Vladykin N.V. (2008) Mineralogical peculiarities of the unique carbonatites of Beriah River. Pp. 77–79 in: *Geochemistry of Magmatic Rocks: Alkaline Magmatism of Earth* (L.N. Kogarko, editor). GEOKhI, St. Petersburg, Moscow [abstract, in Russian].

Krmíček L., Cempírek J., Havlín A., Přichystal A., Houzar S., Krmíčková M. and Gadas P. (2011) Mineralogy and petrogenesis of a Ba–Ti–Zr-rich peralkaline dyke from Sebkovice (Czech Republic): recognition of the most lamproitic Variscan intrusion. *Lithos*, **121**, 74–86.

Kullerud K (1995) Chlorine, titanium and barium-rich biotites: factors controlling biotite composition and implications for garnet-biotite geothermometry. *Contributions to Mineralogy and Petrology*, **120**, 42–59.

Kullerud K (1996) Chlorine-rich amphiboles: interplay between amphibole composition and an evolving fluid. *European Journal of Mineralogy*, **8**, 355–370.

Kullerud K., Zozulya D., Bergh S.G., Hansen H. and Ravna E.J.K. (2011) Geochemistry and tectonic setting of a lamproite dyke in Kvaløya, North Norway. *Lithos*, **126**, 278–289.

Kullerud K., Zozulya D. and Ravna E. (2012) Formation of baotite – a Cl-rich silicate-together with fluorapatite and F-rich hydrous silicates in the Kvaloya lamproite dyke, North Norway. *Minerlogy and Petrology*, **105**, 145–156.

Kumar A., Heaman L.M. and Manikyamba C. (2007) Mesoproterozoic kimberlites in south India: A possible link to 1.1 Ga global magmatism. *Precambrian Research*. **154**(3–4), 192–204.

Kumar A., Ahmed S., Priya R. and Sridhar M. (2013) Discovery of lamproites near Vattikod area, NW margin of the Cuddapah basin, Eastern Dharwar craton, southern India. *Journal of the Geological Society of India*, **82**, 307–312.

Liferovich R.P. and Mitchell R.H. (2005) Composition and paragenesis of Na-, Nb-, and Zr-bearing titanite from Khibina, Russia, and crystal structure data for synthetic analogues. *The Canadian Mineralogist*, **43**, 795–812.

Mitchell R.H. (1989) Compositional variation of micas from the Leucite hills lamproites. *28ᵗʰ International Geological Congress, Washington*. Extended Abstract 2, pp.446–447.

Mitchell R.H. (1995) *Kimberlites, Orangeites, and Related Rocks*. Plenum press. New York, 410pp.

Mitchell R.H. (2006) Potassic magmas derived from metasomatized lithospheric mantle: Nomenclature and relevance to exploration for diamond-bearing rocks. *Journal Geological Society of India*, **67**, 317–327.

Mitchell R.H. and Bergman S.C. (1991) *Petrology of Lamproites*. Plenum Press, New York, 447pp.

Mitchell R.H. and Fareeduddin (2009) Mineralogy of peralkaline lamproites from the Raniganj Coalfield, India. *Mineralogical Magazine*, **73**, 457–477.

Mitchell R.H. and Tappe S. (2010) Discussions of 'Kimberlites and aillikites as probes of the continental lithospheric mantle'. *Lithos*, **109**, 72–80.

Murphy D.T., Collerson K.D. and Kamber B.S. (2002) Lamproites from Gaussberg, Antarctica: Possible transition zone melts of Archaean subducted sediments. *Journal of Petrology*, **43**, 981–1001.

Neelkantam S. (2001) Exploration for diamonds in southern India. *Geological Survey of India Special Publication*, **58**, 521–555.

Nemec D. (1987) Baotite – a rock-forming mineral of Ba-rich hyperpotassic dyke rocks. *Neues Jahrbuch Mineral Monatshefte*, **1**, 31–42.

Nowell G.M., Pearson D.G., Bell D.R., Carlson R.W., Smith C.B., Kempton P.D. and Noble S.R. (2004) Hf isotope systematics of kimberlites and their megacrysts: New constraints on their source regions. *Journal of Petrology*, **45**, 1583–1612.

Obodda H.P. and Leavens P.B. (2004) Zagi mountain – Northwest frontier province, Pakistan. *Mineralogical Records*, **35**, 205–220.

Peng C.J. (1959) The discovery of several new minerals of rare elements. *American Mineralogist*, **45**, 7–45

Potter E.G. and Mitchell R.H. (2005) Mineralogy of the Deadhorse Creek volcaniclastic breccia complex, northwestern Ontario, Canada. *Contributions to Mineralogy and Petrology*, **150**, 212–229.

Prelevic D., Foley S.F., Romer R.L. and Conticelli S. (2008) Mediterranean Tertiary lamproites derived from multiple source components in postcollisional geodynamics. *Geochimica et Cosmochimica Acta*, **72**, 2125–2156.

Rapp R.P., Irifune T., Shimizu N., Nishiyama N., Norman M.D. and Inoue J. (2008) Subduction recycling of continental sediments and the origin of geochemically enriched reservoirs in the deep mantle. *Earth Planetary Science Letters*, **271**, 14–23.

Rudashevsky V.N., Gorkovetz V.Ya., Rudashevsky N.S., Popov M.G. and Raevskaya M.B. (2011) Lamproites of the Kostomuksha ore area, West Karelia (mineralogy and 3D-method of investigation). Pp. 167–168 in: *Ore Potential of Alkaline, Kimberlitic and Carbonatitic Magmatism* (L.N. Kogarko, editor). Pravo i economica, Moscow – Minsk [abstract, in Russian].

Semenov E.I., Khun V.S. and Kapitonova T.A. (1961) Baotite, a new niobian mineral. *Doklady AN USSR*, 136, 915–916 [in Russian].

Shaikh A.M., Kumar S.P., Patel S.C., Thakur S.S., Ravi S. and Behera D. (2018) The P3 kimberlite and P4 lamproite, Wajrakarur kimberlite field, India:

mineralogy, and major and minor element compositions of olivines as records of their phenocrystic vs xenocrystic origin. *Mineralogy and Petrology*, 11ᵗʰ *IKC volume*, **112**(Suppl 2), 609, https://doi.org/10.1007/s00710-018-0562-2

Shaikh A.M., Patel S.C., Ravi S., Behera D. and Pruseth K.L. (2017) Mineralogy of the TK1and TK4 'kimberlite' in the Timmasamudram cluster, Wajrakarur Kimberlite Field, India: Implications for lamproite magmatism in a field of kimberlites and ultramafic lamprophyres. *Chemical Geology*, **455**, 208–230.

Shuriga T.N., Ryabeva E.G. and Dubakina L.S. (1980) Baotite – a new finding in the USSR. *Doklady AN SSSR*, **252**, 1220–1223 [in Russian].

Sridhar M. and Rau T.K. (2005) Discovery of a new lamproite field Ramadugu lamproite field (RLF), Nalgonda District, Andhra Pradesh. *Proceedings of the Group Discussion on Kimberlites and Related Rocks of India*. Organised by the Geological Society of India, Bangalore, pp. 55–57 [Extended abstracts].

Tainton K.M. and Mckenzie D. (1994) The generation of kimberlites, lamproites and their source rocks. *Journal of Petrology*, **35**, 787–817.

Talukdar D., Pandey A., Chalapathi Rao N.V., Kumar A., Belyatsky B. and Lehmann B. (2018) Petrology and geochemistry of the Mesoproterozoic Vattikod lamproites, Eastern Dharwar Craton, southern India: evidence for multiple enrichment of sub-continental lithospheric mantle and links with amalgamation and break-up of the Columbia supercontinent. *Contributions to Mineralogy and Petrology*, **173**, 67, https://doi.org/10.1007/s00410-018-1493-y

Tappe S., Foley S.F., Stracke A., Romer R.L., Kjarsgaard B.A., Heaman L.M. and Joyce N. (2007) Craton reactivation on the Labrador sea margins:40Ar/39Ar age and Sr-Nd-Hf-Pb isotope constraints from alkaline and carbonatites intrusive. *Earth and Planetary Science Letters*, **256**, 433–454.

Tappe S., Pearson D.G. and Prevelic D. (2013) Kimberlite, carbonatite, and potassic magmatism as part of the geochemical cycle. *Chemical Geology*, **353**, 1–3.

Tappe S., Smart K., Torsvik T., Massuyeau M. and de Wit M. (2018*a*) Geodynamics of kimberlites on a cooling Earth: clues to plate tectonic evolution and deep volatile cycles. *Earth Planet Science Letters*, **484**, 1–14.

Tappe S., Dongre A., Liu C.Z. and Wu F.Y. (2018*b*) 'Premier' evidence for prolonged kimberlite pipe formation and its influence on diamond transport from deep Earth. *Geology*, **46**, 843–846.

Tommasini S., Avanzinelli R. and Conticelli S. (2011) The Th/La and Sm/La conundrum of the Tethyan realm lamproites. *Earth and Planetary Science Letters*, **301**, 469–478.

Wagner C. and Velde D. (1986) The mineralogy of K-richterite-bearing lamproites. *American Mineralogist*, **71**, 17–37.

Wall F., Williams C.T. and Woolley A.R. (1996) Pyrochlore from weathered carbonatites at Lueshe, Zaire. *Mineralogical Magazine*, **60**, 731–750.

Woolley A.R., Bergman S.C., Edgar A.D., LeBas M.J., Mitchell R.H., Rock N. and Scott Smith B. (1996) Classification of lamprophyres, lamproite, kimberlite and the kalsilitic, melilitic, and leucitic rocks. *The Canadian Mineralogist*, **34**,175–186.